Mapping Structures that Control Contaminant Migration using Helicopter Transient Electromagnetic Data

Louise Pellerin[1], Les P. Beard[2] and Wayne Mandell[3]
[1]Green Engineering, Inc., 2215 Curtis St., Berkeley, Calif. 94702
Email: pellerin@ak.net
[2]Battelle-Oak Ridge Operations, 105 Mitchell Road, Suite 103, Oak Ridge, Tenn. 37830
[3]Army Environmental Command (Retired), Greenville, N.C. 27858

ABSTRACT

Tooele Army Depot, Tooele County, Utah has developed a hydrogeological model to predict spatio-temporal changes in trichloroethylene contamination originating from sources on the base. Established in 1942 to store World War II supplies, ammunition, and combat vehicles, the Depot is situated in the Basin and Range Providence about 50 km west of Salt Lake City, Utah. In order to better define this hydrogeological framework, a helicopter-borne, time-domain electromagnetic system, known as SkyTEM, was used to survey a 64-km^2 area of the Depot. Areas where carbonate basement is known from prior studies to be at or near the surface were clearly delineated in the SkyTEM data as a high resistivity zone, which begins near the ground surface and continues to the deepest samples at about 200 m. In some places the basement appears to be conductive rather than resistive. In areas where unconsolidated sedimentary cover is known to be thick, such as in the northwest part of the survey area, resistivities were low throughout the sample intervals. The SkyTEM data supports the existence of some, but not all, of the hydrological boundaries hypothesized from potentiometric information. Shallow high-resistivity layers in the east and southeast portions of the survey area appear to be underlain by more conductive sediments, and so should not necessarily be interpreted as shallow bedrock, but possibly as resistive sediments such as dry sand and gravel. One of the most significant results of the survey is the delineation of a narrow unit, interpreted as a paleochannel, at depths greater than 100 m that may be responsible for migration of contamination to the northwest.

Introduction

An airborne transient electromagnetic survey was carried out over an area of 64 km^2 at the Tooele Army Depot (TEAD), Tooele County, Utah to better define geological structures and hydrogeological units in the surveyed area. Survey results were meshed with existing geological and hydrological data to improve the TEAD hydrogeological model. SkyTEM, a unique airborne transient electromagnetic sounding system developed in Denmark and designed specifically to address hydrogeological problems (Sørensen and Auken, 2004), was used for the survey.

The Tooele Ordnance Depot was established in 1942, and in World War II was a storage depot for supplies, ammunition, and combat vehicles (see www.tooele.army.mil). In 1962, the post was renamed the Tooele Army Depot. TEAD is currently responsible for shipping, storage, maintenance, and demilitarization of conventional ammunition. Activities related to these missions resulted in groundwater contamination, in particular contamination from trichloroethylene (TCE). A groundwater flow and contaminant transport model was developed by Fenske *et al.* (2005) to better mitigate any hazard to the public that might be associated with the contamination.

Site Geology and Hydrogeology

The Tooele Army Depot lies in the Tooele Valley, and is located about 55 km southwest of Salt Lake City. The Tooele Valley is a Basin-and-Range structural depression that comprises an area of over 700 km^2. It is filled with unconsolidated and partly-consolidated sediments of Paleogene and Neogene ages. These sediments range from gravels to clays, and represent a variety of depositional environments. Basin fill sediments thicken to the north, and are reported to have a thickness greater than 3,000 m in the north-central part of the valley (Stokes, 1988). In the area of the SkyTEM survey, sediment thicknesses range from zero at a bedrock outcrop to hundreds of meters throughout much of the surveyed area.

Bedrock units consist of Paleozoic quartzite, sandstone, limestone, and dolomite. Bedrock over much of the survey area is covered by thick sediments, but a limestone outcrop about 2 km northwest of the Utah Industrial Depot suggests shallow bedrock over some portion of the survey area. Drilling and geophysical studies suggest a fault-bounded, uplifted, tilted fault block dipping sharply to the north-northwest (Asch, 2005). The location of the SkyTEM survey area is shown by the dashed square in Fig. 1, which also shows groundwater flow direction (Susong, 1999). The proposed uplifted fault block lies approximately in the center of the SkyTEM survey area. In addition, dramatic changes in water levels over short lateral distances suggest other faults in the study area (Fenske *et al.*, 2005). The hypothesized faults splay off from the uplifted bedrock block, and their inferred locations are also shown in Fig. 1 along with the location map and the SkyTEM survey area.

Groundwater flow and hydraulic head at TEAD is governed by fractures in bedrock, highly transmissive alluvium in the north, low-permeability fault zones, and less hydraulically conductive alluvium in the south. Drawdown data from pump tests indicate that the uplifted bedrock block may be encased by hydraulically low-permeability material, probably the result of fault gouge or the weathering of carbonates into low-permeability clays. Considerable detail on the groundwater conditions at TEAD can be found in Fenske *et al.* (2005). Brackish to briny waters may be found in deeper units in the survey area, overlain by multiple fresh water aquifers. Brines would typically make a geological unit appear less electrically resistive than the same unit, were it to contain fresh water.

The direction of groundwater flow is across the TEAD site, as shown in Fig. 1 (Susong, 1999). Elevation of the water table varies from ~4,470 ft (~1,355 m) on the southern boundary to ~4,285 ft (~1,300 m) on the northwestern boundary of the TEAD; the depth to ground water ranges from to 120 ft (~36 m) to 375 ft (~115 m). A drop of the hydraulic gradient across the site is relatively flat (0.001), but large gradients exist. The sources of these gradients are presumed to be faults or other types of hydrogeological boundaries.

The TEAD site was divided into four hydraulic units by Fenske *et al.* (2005): 1) fractured bedrock that dominates the central and southern portions of the site, 2) highly transmissive alluvium to the north, 3) shallow alluvium to the south, and 4) fault zones. Abrupt head

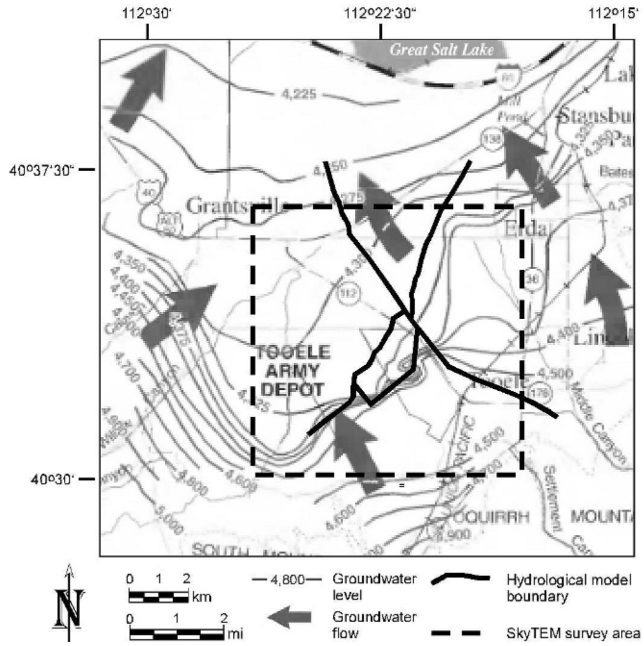

Figure 1. The SkyTEM survey area at the Tooele Army Depot delineated by dashed black lines; faults or unit boundaries, derived from previous hydrological studies, are shown in bold black lines (from Fenske *et al.*, 2005); and groundwater flow indicated by arrow.

changes occur at faults and, as such, are controlling features. Uplifted bedrock exhibits behavior characteristic of fracture-low environments. Delimitation of the encased bedrock is an important hydrogeologic parameter controlling TCE plume migration. The northern alluvium is several interconnected aquifer systems loosely bound by discontinuous fine-grain sediments. Total dissolved salts (TDS) vary from 500 milligrams per liter in the center east of the SkyTEM survey area to >2,000 milligrams per liter near the northeast corner (Susong, 1999). The latter values are consistent with brine and the TDS will most likely increase to the north to closer proximity to the Great Salt Lake.

The simplified hydrogeological model, showing hydraulic boundaries at 225 ft (~70 m), was calibrated by matching the total changes in water levels and the shape of the recovery curve (Fenske *et al.*, 2005) from long-term pump tests. Changes in horizontal hydraulic conductivity primarily affected the total simulated head change over a given time interval. The changes in vertical hydraulic conductivity and specific storage primarily affected the initial rebound following shutdown, and the changes in specific yield/porosity primarily affected the slope of the recovery curve.

The modeled TCE plume and observed concentrations in μg/L are shown in Fig. 2. Although observations are sparse to the east, it is clear that there

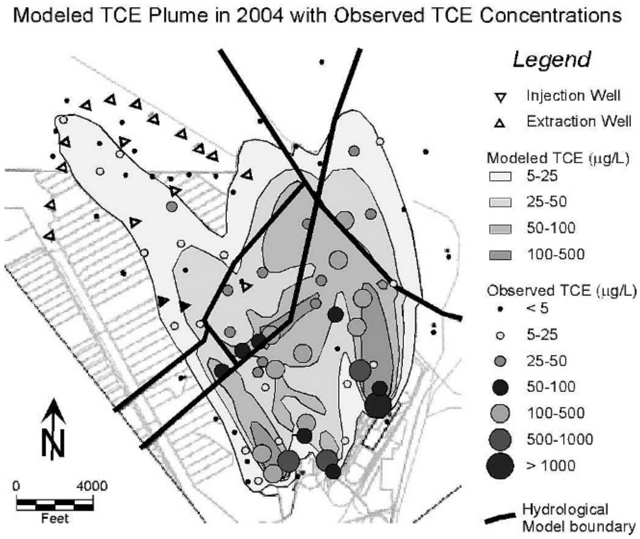

Figure 2. The hydrological-modeled TCE plume shown with observed concentrations from 2004. The bold lines define the modeled hydrogeological units from Fenske *et al.* (2005).

are two plumes: the main plume extends to the northwest and the northeastern boundary plume to the north (Fenske *et al.*, 2005). The northeast-southwest trending modeled fault (Fenske *et al.*, 2005) is a barrier to eastward flow.

SkyTEM Airborne Geophysical System

SkyTEM is a time-domain, electromagnetic (TEM) helicopter system specifically designed for mapping geological structures for groundwater and environmental investigations, and was developed as a rapid alternative to ground-based TEM surveying (Sørensen and Auken, 2004). The entire system is carried independently of the helicopter as a sling load, as shown in Fig. 3. The SkyTEM system is able to acquire very accurate data because of low internal noise and virtually no drift. SkyTEM uses a unique dual transmitter for a helicopter system, combining low transmitter magnetic moment for high vertical resolution in the near surface with high moment for increased depth of investigation, to about 250 m. This is in contrast to single-moment commercial systems, which give up near-surface resolution for deep penetration. Additional technical details of the system can be found in Appendix A.

The transmitter and receiver coils, power supplies, laser altimeters, GPS, electronics, and data logger are carried as a sling load from the cargo hook of the helicopter. Operational parameters and selected data "snapshots" are transmitted real time to a geophysicist on the ground. The transmitter, mounted on the lightweight wooden lattice frame, is a 283 m^2 multi-turn loop with variable magnetic moment to increase the system's dynamic range. The receiver is rigidly mounted on the side of the transmitter loop in a location that minimizes interference from the transmitted field, with a 2-m vertical offset. Hence, this configuration can be compared to the common central-loop TEM configuration and the data can be processed and inverted as such. Most system parameters are user defined and therefore various strategies can be applied to optimize a given survey.

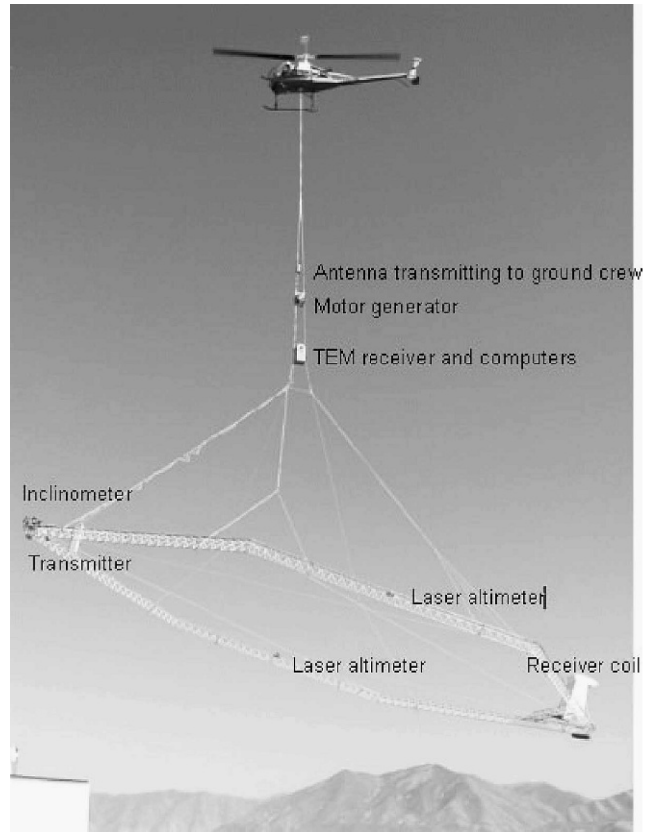

Figure 3. Photograph of SkyTEM in operation during the TEAD survey. Key elements of the system are labeled. Once survey speed is attained the frame is stable to within 10 degrees of horizontal and the attitude is recorded.

The flight speed and altitude of the system are key factors in defining the lateral resolution as well as the number of averaged datasets for a satisfactory signal-to-noise ratio. The SkyTEM system is configured with both the transmitter and the receiver as close to the ground as possible to give the largest signal and the best resolution. The SkyTEM system is flown as low as possible; in the TEAD survey the transmitter altitude was approximately 20 m above ground level.

Tooele Army Depot SkyTEM Survey

The data acquisition area for the SkyTEM survey was an 8-km × 8-km (5-mi × 5-mi) block encompassing the Utah Industrial Depot, about 40% of the ordnance storage area, and the entirety of the well injection field described in Fenske *et al.* (2005), as shown Fig. 4. The survey covered approximately 200 line-kilometers of data, and was carried out from October 19–21, 2005. The survey was flown with a nominal line spacing of 200 m. A large section of the southeast quadrant of the area could not be flown safely because of industrial or residential buildup. Additional infill lines were flown in the area directly north of the Utah Industrial Depot to better define the geoelectrical section in an area where faults were thought to be responsible for abrupt changes in measured groundwater level. Over this area of about 1.5 mi × 1.5 mi (2.4 km × 2.4 km), the nominal line spacing was 100 m. Aircraft ground speed was maintained at approximately 15 m/s (30 knots).

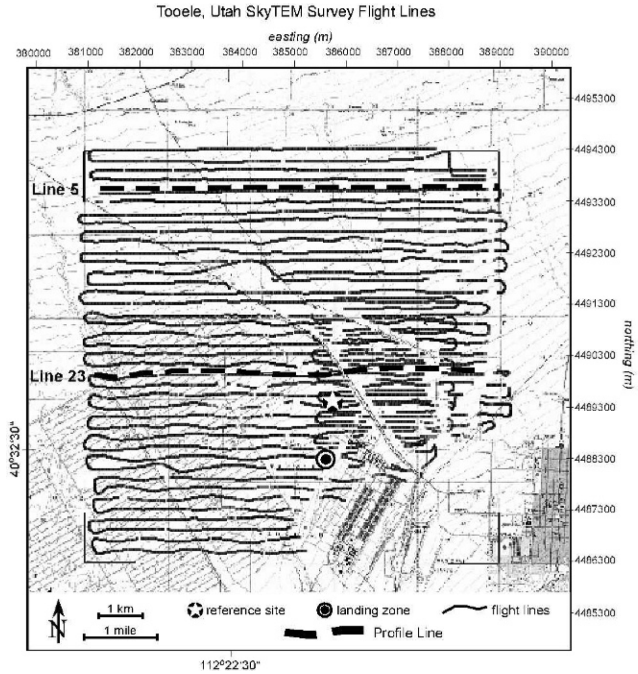

Figure 4. The SkyTEM Tooele, Utah survey area showing the flight lines and two selected profiles as bold dashed lines (referred to in Figure). The underlying topographic map highlights infrastructure in the survey area such as roads, power lines, and the industrial depot.

Resistivity Maps and Profiles

Data were processed with the Aarhus Workbench software package (Aarhus Geophysics, 2009) developed by the Hydrogeophysics Group of the University of Aarhus, Denmark. The substantial amount of data includes GPS, tilt and altitude, in addition to system status and voltage data. The transient data are processed with automatic filters and manual editing. Sign and slope filters were used to cull data when sign changes were detected, as in the presence of cultural features such as power and pipelines (Auken *et al.*, 2004), or if the slope of the data curve was not within two specified slopes. A fairly limited slope band centered at ~0.4 was used with the hopes of culling the response caused by buried munitions, however manual editing was necessary to remove shallow TEM responses caused by ordnance-filled revetments in the SW corner of the survey area. Data were averaged using a trapezoid filter, thereby increasing the signal-to-noise ratio at late times where the signal level is relatively low while maintaining a high resolution at earlier times, where signal levels are relatively high. An averaged sounding consists of ten SkyTEM transients yielding data from 10 microseconds to up to 9 milliseconds.

In the second step, sounding data are inverted thereby transforming the data from voltages as a function of time to resistivities as a function of depth (Fig. 5). A sounding consists of low- and high-moment segments, which are two distinct datasets. Because the two segments are slightly separated spatially, the data sequences are inverted with somewhat different locations and corresponding altitudes. The high- and low-moment data sequences are inverted using Mutually Constrained Inversion (MCI) as discussed in Auken *et al.* (2001) and shown in Fig. 5. This approach allows for the different flight altitudes and any small model discrepancies between the two spatially separated segments. Laterally Constrained Inversion (LCI) is used from sounding to sounding so that the models vary smoothly over small distances. The one-dimensional (1-D) inverse models are used to construct resistivity interval plan view maps at depths from 0 to 220 m.

Eight depth interval resistivity slices are shown in Fig. 6. The top slice covers only the first 20 m below the ground surface, but some structures of geological significance can be seen. The uppermost unit in the NW quadrant has low earth resistivities characteristic of saturated sediments with a high TDS content, which is consistent with a low hydraulic gradient in proximity to the Great Salt Lake. Low resistivities also appear in the southwestern quadrant, and are likely of geologic origin, *i.e.*, fluvial deposits. A high resistivity zone can be seen trending from southwest to northeast through the central portion of the survey area. This trend is in agreement with geological models purporting an elevated bedrock block. In fact, the bedrock block outcrops in this zone, about 1-km west from the reference site, designated by a star in Fig. 4 and Fig. 6. The unit corresponds to the fractured bedrock unit defined in the hydrological modeling. The eastern part of the survey area appears to be the most resistive, possibly reflecting

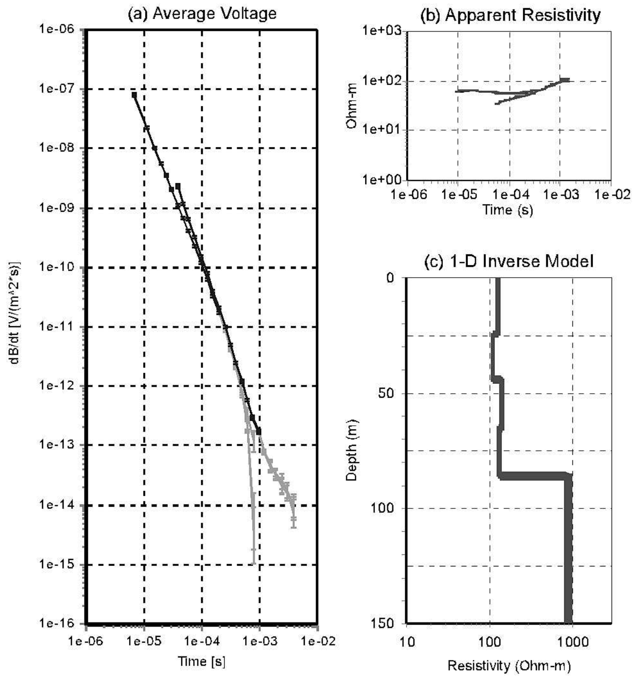

Figure 5. (a) Average voltage data with masked data in light gray, (b) corresponding apparent resistivity from the edited voltage, and (c) 1-D inverse models. The dots represent data in (a) and (b), while the smooth curve is the response of models in (c).

drier and possibly less saline near-surface conditions than are encountered in the northwest.

The electrical character changes with increasing depth. The NW quadrant still shows low resistivities, indicative of the thick sediment package in this area. The SW-NE trend of the bedrock high is more apparent, and appears to extend further to the southwest than in the 0–20 m depth interval. The sizeable area of low resistivities in the shallowest interval in the SW quadrant has been reduced to a small circular feature. This low resistivity unit persists to the deepest resistivity interval and could indicate an upwelling of saline fluids. This response being caused by a shallow anthropomorphic conductive feature was rejected because the responses of the buried ordnance were clearly visible and culled in the voltage data, and there was no evidence of other structure of the scale responsible for the anomaly.

Interpretation

The primary geological structures to be defined with the SkyTEM survey data are: depth to basement, or its corollary, sediment thickness; locations of major faults or hydrological unit boundaries; and preferred groundwater flow paths. The pertinent structures are interpreted from the depth interval maps of Fig. 6.

Depth to Bedrock

The bedrock has no consistent resistivity signature. The shallow bedrock horst near the center of the SkyTEM survey area appears electrically resistive, a characteristic that would be compatible with a carbonate formation. However, in many resistivity cross-sectional profiles the lowermost electrical layer appears conductive, and is deeper than boreholes that sampled to depths of ~100 m, therefore the lithology and degree of compaction is uncertain.

Resistivity cross-sections were derived from 1-D LCI models (Auken *et al.*, 2005) along the SkyTEM profiles depicted in Fig. 4, and can be used to illustrate the changes in geology from north to south in the surveyed area. Figure 7 shows resistivity cross-sections from two east-west profiles. The topmost profile is located in Fig. 4, and shows the thick conductive unconsolidated sediments in the north part of the area. The western three-fourths of the profile show conductive sediments that extend at least as deep as the SkyTEM system was able to sample, about 200 m below ground level. At position x = 6,000 m the resistivity section becomes more complex than the predominantly conductive section, and the resistive zone at 6,500 m corresponds to the northeast trending fault splay predicted by the hydrological modeling (Fenske *et al.*, 2005) shown in the maps of Fig. 6. Line 23, the lower panel in Fig. 7, is about 3,800 m south of Line 5 and passes over the shallow bedrock carbonate horst in the center of the survey area. A dense dolomite outcrop in the area suggests a horst, as does gravity data. The horst appears as a shallow resistive zone that continues to the maximum SkyTEM sampling depth; west of this zone a resistive layer overlies a more conductive zone. Because of the local stratigraphy we interpret the resistive layer as dry, less saline unconsolidated valley fill, rather than carbonate bedrock.

Deeper in the fill the moisture and salinity content increases, and the resistivity decreases. East of the horst, the electrical section is more complex and the unconsolidated sediments remain resistive through the entire depth section, probably indicative of less saline conditions than in the west. The blanked out areas in both profile cross-sections are where the helicopter had to fly high to avoid power lines or other buildings, and the data were not deemed reliable.

Evidence of Faulting

Few bedrock outcrops occur in the SkyTEM survey area, and most faulting was inferred from borehole potentiometric measurements and subsequent modeling (Asch, 2005; Fenske *et al.*, 2005). A number of faults inferred from head levels modeled from potentiometric data are superimposed on the depth sections in

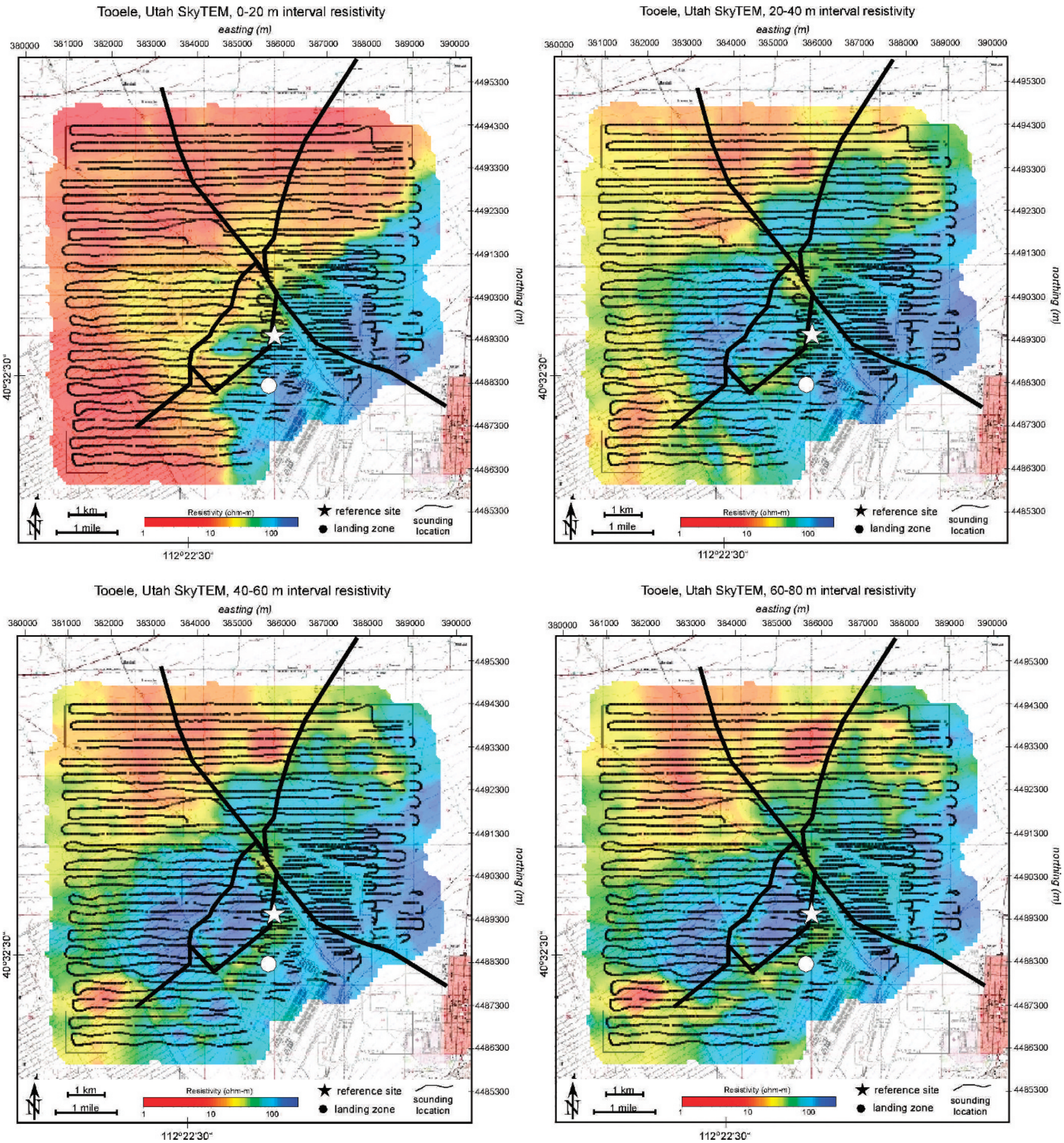

Figure 6. Estimated resistivity over eight depth intervals from 0 m to 190 m. The unit boundaries (faults) defined by hydrological modeling are superimposed (bold black lines) as a visual aid to estimate the changes in electrical resistivity boundaries with depth.

Fig. 6. Major faults are inferred to splay from the shallow bedrock block in the center of the survey area. Most of these inferred fault splays are only partially supported by the SkyTEM survey data. Abrupt resistivity changes that might indicate faulting are absent in the 0–20 m interval, indicating that faulting does not occur in the near-surface or that there are no measurable resistivity contrasts across fault boundaries.

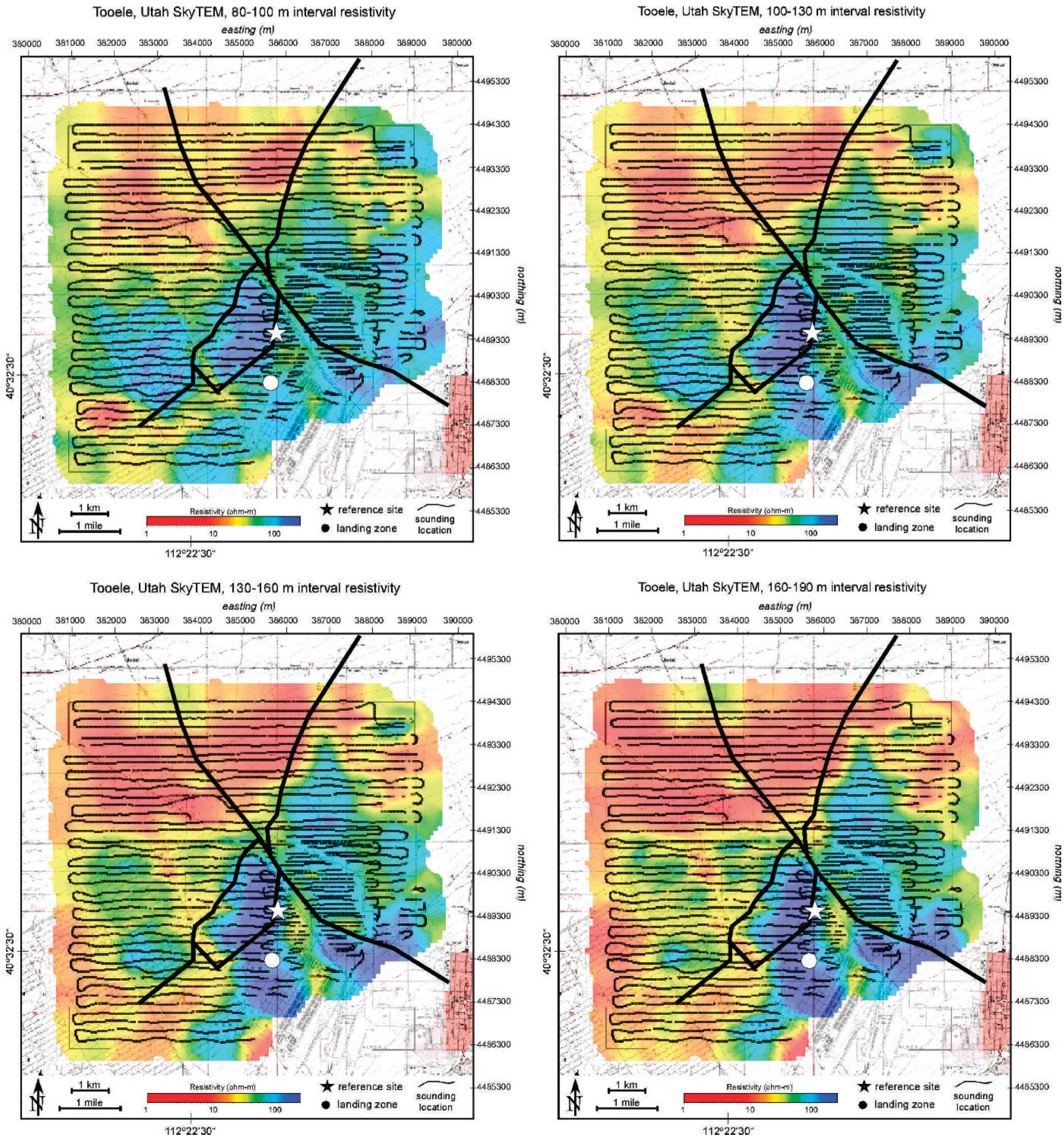

Figure 6. Continued.

Deeper resistivity sections clearly image the shallow bedrock block, and the sharp resistivity gradients around the block support the hypothesis of faults surrounding the block. Resistivities along the proposed fault, which splay to the SW from the upraised bedrock block, also show sharp contrasts, consistent with faulting. However, sharp resistivity contrasts cannot be correlated with the proposed NW-SE trending fault. As mentioned previously, this absence of resistivity evidence does not rule out the possibility of faults in these locations, but other possible causes for hydrological head drops should be examined as well.

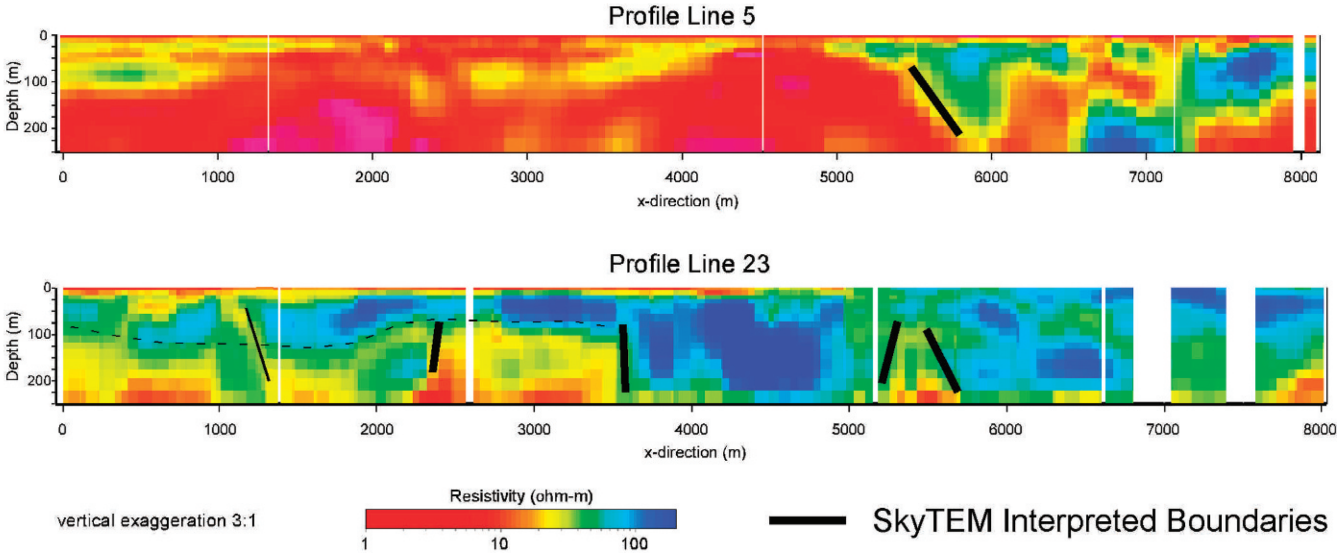

Figure 7. Resistivity depth sections for profile lines 5 and 23, as shown in Figure. Thick conductive sediments are apparent in red in the top profile (Profile 6); a resistive limestone horst (blue) is centered in the lower profile (Profile 23).

The SkyTEM data indicate sharp resistivity contrasts, as depicted by the bold black lines in Fig. 8(a). These contrasts could be related to undiscovered faulting, or indicate different geometries for some of the already proposed faults, as with, for example, the NNE trending fault in the top right quadrant. Some of these features warrant follow up investigations.

Contaminant Pathway

Figure 8(b) shows the resistivity model at a depth of 130–160 m with the major contours of the TCE plume superimposed as dashed lines. The conductive structure, probably fluvial, leading to the NW corresponds to the finger of the plume that is mapped approximately perpendicular to general groundwater flow to the northeast. A paleochannel, being filled with sand and gravel, is often seen as an electrically resistive structure. However, in this case, intrusion of brine-rich water to the north combined with high porosities in the channel could result in the conductive response of this pathway (Macaulay, 2006).

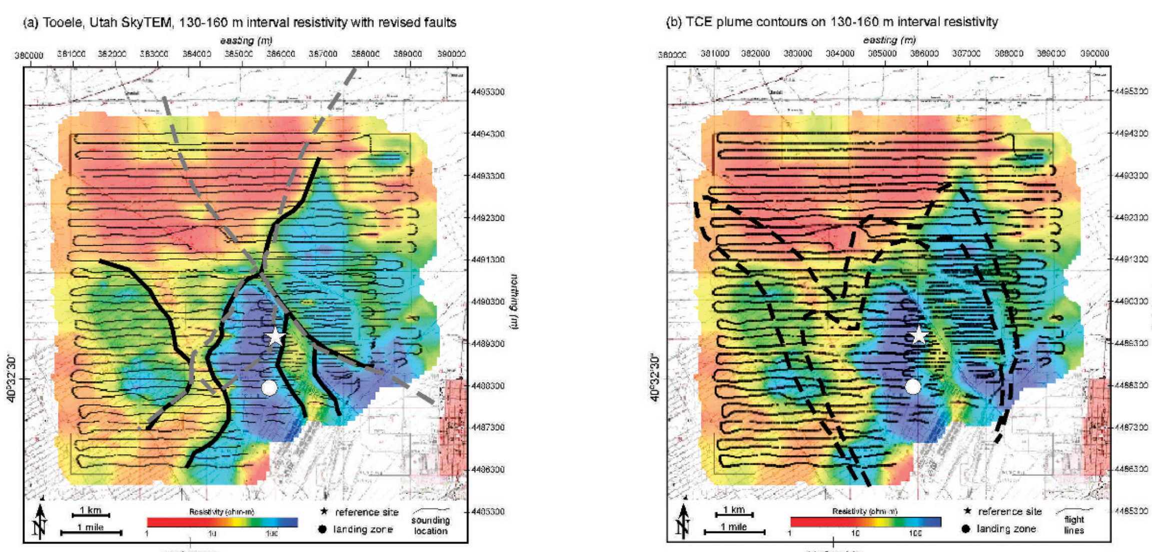

Figure 8. Estimated resistivity over depth interval 130–160 m with (a) interpreted faults derived from SkyTEM data in bold black lines and the unit boundaries derived from hydrological modeling in dashed gray lines, and (b) outer contours of TCE plume at 5–25 and 25–50 μG/L denoted with long and short-dashed lines, respectively.

Conclusions

The SkyTEM survey was the first wide-area geophysical survey at TEAD, and serves as a framework for integration of other TEAD data. The SkyTEM data were of good quality and self-consistent. Data collected at the calibration site were repeatable. There appears to be good correlation of SkyTEM earth resistivity estimates with known geology. Areas where basement is known to be from prior studies at or near the surface were clearly delineated in the SkyTEM data as a high resistivity zone, which begins near the ground surface and continues to the deepest samples. In some places, basement may be conductive rather than resistive. In the northwest part of the survey area, resistivities were low throughout the sample intervals that are consistent with brine saturation in proximity to the Great Salt Lake.

The SkyTEM data supports the existence of some, but not all, of the faults that have been proposed based on potentiometric studies. Although faults are a difficult target for most geophysical methods, a few fault-like structures defined by electrical resistivity contrasts appear besides those that were based on groundwater head data and modeling. Shallow high-resistivity layers in the east and southeast portions of the survey area appear to be underlain by more conductive sediments, and so should not be interpreted as shallow bedrock. One of the most significant results of the survey is the delineation of a conductive unit, interpreted as a paleochannel at depths >100 m in which brine may have migrated from the north. We suggest structure may be responsible for transport of the TCE contamination.

Acknowledgements

The authors wish to thank Jan Steen Joegensen, Lars Jensen and Max Halkjaer of SkyTEM Aps for the data acquisition, David Beard of Dragonfly Air for his excellent flying, Carl Cole, U.S. Army Corps of Engineers for providing invaluable logistical assistance and geological advice before and during the SkyTEM survey, and Esben Auken, Hydrogeophysics Group, University of Aarhus, DK, for his assistance with the processing and inversion software. We also thank Greg Hodges, an anonymous reviewer and the JEEG associate editor Antonio Menghini for their thoughtful comments that improved the paper.

References

Aarhus Geophysics, 2009, Aarhus Workbench Guide to Processing and Inversion of SkyTEM Data: www.aarhusgeo.com, 41 pp.

Asch, T., 2005, Summary and integration of geophysical investigations of the Tooele Army Depot (TEAD), Tooele, Utah: USGS Open-File Report 1338-2005, 53 pp.

Auken, E., Christiansen, A.V., Jacobsen, B.H., Foged, N., and Sørensen, K.I., 2005, Piecewise 1D Laterally Constrained Inversion of Resistivity Data: Geophysical Prospecting, **53**, 497–506.

Auken, E., Pellerin, L., and Sørensen, K., 2001, Mutually Constrained Inversion (MCI) of Electrical and Electromagnetic Data: *in* Expanded Abstracts: Annual International Meeting, Society of Exploration Geophysics 1455–1458.

Auken, E., Halkjær, M., and Sørensen, K.I., 2004, SkyTEM—Data Processing and a Survey: *in* Proceedings: Symposium on the Application of Geophysics to Engineering and Environmental Problems (SAGEEP), Colorado Springs, Colorado, USA.

Fenske, J., Grogin, L., and Andersen, P., 2005, Tooele Army Depot Groundwater Flow and Contaminant Transport Model: U.S. Army Corps of Engineers, Sacramento District, Environmental Engineering Branch, PR-59.

Macaulay, S., 2006, Application of Airborne Electromagnetics to Salt Mapping—3 Australian Case Studies: Symposium on the Application of Geophysics to Engineering and Environmental Problems (SAGEEP).

Sørensen, K.I., and Auken, E., 2004, SkyTEM—A new high-resolution helicopter transient electromagnetic system: Exploration Geophysics, **35**, 191–199.

Stokes, W.L., 1988, The Geology of Utah: Utah Museum of Natural History Occasional Paper, **6**, 280 pp.

Susong, D.D., 1999, Ground-water resources of Tooele Valley, Utah Edition: USGS Library Call Number (200) F327 no.99-125.

APPENDIX A
SkyTEM SPECIFICATIONS

The SkyTEM system used a low and high transmitter moment (Table A-1) and is based on a central-loop array configuration. The transmitter, mounted on a lightweight wooden lattice frame, is a 283 m^2 multi-turn loop with variable moment to increase the system's dynamic range. The shielded, over-damped, multi-turn receiver loop is rigidly mounted on the side of the transmitter loop in a near-null position of the primary transmitted field, which minimizes distortions from the transmitter, with a 2-meter vertical offset. Hence, this configuration can be compared to a central-loop configuration and the data are processed and inverted as such. The transmitter is powered by a motor generator, which is placed between the helicopter and the frame. It uses a combination of high and low transmitter moments for high vertical resolution in the near surface and increased depth of investigation to $\sim$250 m. The dual moment array has the advantage of being able to attain measurements of time gates shown in Table A-2.

With the system repetition frequencies, a complete measurement cycle, including both the low and the high moment dataset, takes about 2 s. Hence, there is high data density along the flight line and several soundings can be averaged in a running mean to enhance data quality.

The transmitted current is measured for each data set at each moment; the exact value depends on the ambient outdoor temperature. The complete waveform is then scaled due to the variations caused by temperature variations.

The transmitter waveform can be described as a modified square wave where the current builds quickly and then turned off within a few microseconds. The very fast turn-off time of the low-moment transmitter results in higher vertical resolution of the upper layers. Enhanced resolution of the upper layers results in better resolution at depth and a greater depth of investigation.

High-altitude measurements are used to demonstrate that there is no bias in the system. Data are acquired with the system at more than 1,000 m above the ground, but with the transmitter off as shown in Fig. A-1. By comparing the received signal from the transmitted current and the ambient noise, it is clear no signal is left in the instrumentation that will disturb the earth signal when flying at production altitude.

Two independent 9 Hz laser altimeters, with an accuracy of 10 cm within an altitude envelope of 1.5 m to 135 m, are used for navigation. The tilt angle of the frame is measured in two perpendicular directions at a frequency of 2 Hz. There is no data distortion for tilt angles <10 degrees. From 10–20 degrees distortions are corrected in the processing. In general, the frame is extremely stable and tilt angle of <5 degrees are common for production speeds. Given the low topographic relief and lack of vegetation in the TEAD survey area, the tilt angle was well below 5 degrees at production flight speeds. Two independent GPS receivers provide positioning data with a frequency of about 1 Hz and an accuracy of 1–2 m. If desired a DGPS with a higher accuracy can be implemented, but was not necessary for the objectives of the TEAD survey.

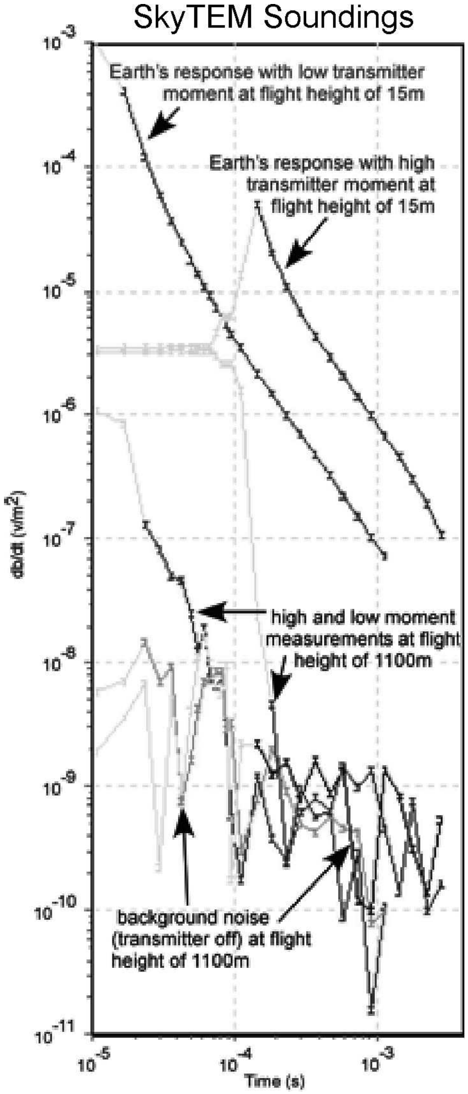

Figure A-1. SkyTEM data acquired at production height compared with data collected at 1,100 m with the transmitter off and on to illustrate the lack of bias in the system.

Table A-1. Characteristics of the low and high moment systems.

Low moment	High moment
1 transmitter turn	4 transmitter turns
Current about 37 A	Current about 95 A
Gate center times from 10 microseconds (defined from the beginning of the turn off at 8.2 microseconds) up to about 1 ms	Gate center times from 50 microseconds (defined from the beginning of the turn off) up to about 5.6 ms
Repetition frequency (on time 800 microseconds, off time 1,280 microseconds) is about 240 Hz	Repetition frequency (on time 10.000 microseconds, off time 6.670 microseconds) is about 30 Hz

Table A-2. The center times, in microseconds, for the measurement gates.

Gate	Time	Gate	Time	Gate	Time
2	10.0	11	111.8	20	911.2
3	16.3	12	145.4	21	1141.0
4	22.8	13	185.2	22	1429.2
5	29.2	14	234.4	23	1791.2
6	35.6	15	295.2	24	2246.0
7	45.2	16	370.6	25	2817.4
8	58.0	17	464.4	26	3535.6
9	71.1	18	581.4	27	4438.8
10	86.8	19	727.8	28	5575.0